

CH_2D^+ , the Search for the Holy GRAIL

Evelyne Roueff,^{*,†} Maryvonne Gerin,[‡] Dariusz C. Lis,[¶] Alwyn Wootten,[§] Nuria
Marcelino,[§] Jose Cernicharo,^{||} and Belen Tercero^{||}

*Observatoire de Paris, Place J. Janssen, 92190 Meudon, France, Département de Physique de
l'ENS, 24 rue Lohmond, Paris 75230 cedex 05, France, MC301-17, Caltech, Pasadena, Ca91125,
USA, NRAO, 520 Edgemont Rd., Charlottesville, Virginia 22903, and 28850 Torrejon de Ardoz.
Madrid. Spain*

E-mail: evelyne.roueff@obspm.fr

*To whom correspondence should be addressed

†LUTH and UMR 8102 du CNRS

‡ENS, LERMA and UMR8112 du CNRS

¶Cahill Center for Astronomy and Astrophysics

§North America ALMA Science Center

||CAB. INTA-CSIC

Abstract

CH_2D^+ , the singly deuterated counterpart of CH_3^+ , offers an alternative way to mediate formation of deuterated species at temperatures of several tens of K, as compared to the release of deuterated species from grains. We report a longstanding observational search for this molecular ion, whose rotational spectroscopy is not yet completely secure. We summarize the main spectroscopic properties of this molecule and discuss the chemical network leading to the formation of CH_2D^+ , with explicit account of the ortho/para forms of H_2 , H_3^+ and CH_3^+ . Astrochemical models support the presence of this molecular ion in moderately warm environments at a marginal level.

Keywords: Astrochemistry – Molecular ion CH_3^+ – Deuterium fractionation – Gas phase chemistry

Introduction

CH_3^+ is recognized as a key polyatomic molecular ion in astrophysical plasmas. It has been found in the innermost coma of comet Halley^{1,2} and is thought to be present both in diffuse and dense molecular clouds.³ Despite its importance, there is a lack of high-resolution spectroscopic data, primarily because of its polymerization in discharges.⁴ Laboratory infrared spectroscopy studies have first been conducted in Oka's group.⁵ More recently, threshold photoionization studies of the methyl radical and its deuterated isotopologues in the 9.5 - 10.5 eV photon energy range have allowed to investigate the vibrational spectroscopy of their corresponding cations by using the easily tunable and powerful sources of radiation, provided by the third generation of synchrotron sources.⁶ Rotational spectroscopy of CH_3^+ , however, cannot be achieved as its fully symmetric D_{3h} ground state planar structure does not allow for a permanent dipole moment.

Deuterium substitution of a hydrogen atom in CH_3^+ breaks the symmetry and allows the presence of a small, but significant 0.3 D dipole moment, which gives potentially observable rotational transitions of CH_2D^+ . Regrettably, the molecule is light and the rotational constants are large,

producing a widely spaced level structure. Two independent recent laboratory studies^{??} have considerably improved our knowledge of the CH_2D^+ rotational spectrum, which is now an entry in the CDMS database (Cologne Database for Molecular Spectroscopy)^{??} (<http://www.astro.uni-koeln.de/cdms/>).

CH_3^+ does not react with molecular nor atomic hydrogen, as the corresponding reactions are highly endothermic. Nevertheless, molecular hydrogen can radiatively associate in a slow reaction where a temporary molecular complex CH_5^+ is formed and stabilized through infrared emission. Alternatively, CH_3^+ can exchange a deuteron with HD, producing CH_2D^+ , and offering an efficient pathway to deuteration, as will be discussed later. It may also react with other abundant neutral molecules, suggesting a natural gas-phase path to molecular complexity.[?]

Spectroscopy of the $\text{CH}_{3-n}\text{D}_n^+$ family

Vibrational and rotational constants

Values of the ν_3 fundamental frequency of CH_3^+ (ref.[?]), ν_1 fundamental frequency of CH_2D^+ and CHD_2^+ (ref.[?]), as well as ν_4 frequency of CH_2D^+ (ref.[?]) have been derived from the infrared vibrational spectrum of these ions performed in the group of Oka. As a four atoms containing species, 6 vibrational modes are involved. For the fully substituted species CH_3^+ and CD_3^+ , the ν_3 stretching and ν_4 bending modes are doubly degenerate. Threshold photoelectron spectroscopy studies with highly tunable radiation sources provided by the new third generation synchrotron facility SOLEIL allow to record the photoionization spectra over a wide range of photoionization energies. All the vibrational frequencies of the methyl radical and its deuterium-substituted forms, as well as those of the corresponding ions have been reported by Cunha de Miranda *et al.*, 2010.[?] Additional theoretical quantum calculations are also documented by these authors.[?]

We display the spectroscopic constants of the different deuterated isotopologues in Table 1. Theoretical harmonic frequencies ν_i^0 of CH_3^+ have also been computed by Keceli *et al.*, 2009[?] and are also reported. Finally, Table 1 also gives the rotational spectroscopic constants of the vibra-

Table 1: Spectroscopic constants of CH₃⁺ and its deuterated isotopologues.

	CH ₃ ⁺	CH ₂ D ⁺	CHD ₂ ⁺	CD ₃ ⁺
electronic state	$\tilde{X}^1A'_1$	$\tilde{X}^1A'_1$	$\tilde{X}^1A'_1$	$\tilde{X}^1A'_1$
point group	D_{3h}	C_{2v}	C_{2v}	D_{3h}
ν_1^0 (cm ⁻¹)	3037 [?]			
ν_1 (cm ⁻¹)	2940 [?]	3005 [?]	3056 [?]	2097 [?]
symmetry	a'_1 symmetric stretch	a_1	a_1	a'_1
ν_2^0 (cm ⁻¹)	1418 [?]			
ν_2 (cm ⁻¹)	1359 ± 7 [?]	2240 [?]	2168 [?]	1085 [?]
symmetry	a''_2 OPLA ^a	A_1	A_1	a''_2
ν_3^0 (cm ⁻¹)	3247 [?]			
ν_3 (cm ⁻¹)	3108 [?]	1389 [?]	1036 ⁽²⁾	2345 [?]
symmetry	e' degenerate stretch	a_1	a_1	e' degenerate stretch
ν_4^0 (cm ⁻¹)	1429 [?]			
ν_4 (cm ⁻¹)	1370 [?]	1299 [?]	1188 [?]	1030 [?]
symmetry	e' degenerate bend	b_1	b_1	e' degenerate bend
ν_5 (cm ⁻¹)		3106 [?]	2356 [?]	
symmetry		b_2	b_2	
ν_6 (cm ⁻¹)		1171 [?]	1281 [?]	
symmetry		b_2	b_2	
A (cm ⁻¹)		9.3686865 [?]	7.25251 [?]	
B (cm ⁻¹)	9.3622 [?]	5.7713018 [?]	4.69046 [?]	4.731 [?]
C (cm ⁻¹)	4.7155 [?]	3.5252332 [?]	2.815470 [?]	2.364 [?]

^a OPLA stands for "Out of Plane Large Amplitude" mode

ν_i^0 stands for theoretical harmonic wavenumber. Experimental values of the fundamental wavenumbers ν_i , when available, are displayed. A, B, C refer to the rotational constants.

tional ground state of the different isotopologues. Figure 1, adapted from Brum *et al.* 1993,[?] summarizes the respective numerical values of the fundamental vibrational frequencies on a wavenumber scale for all deuterated isotopologues of the methyl cation.

Zero Point Energies (ZPEs)

Determining zero point energies (ZPEs) is important for predicting the relative stability of different isotopologues as they can be further used to determine the exothermicity of isotopic exchange reactions. Whereas ZPEs values are well known and documented for diatomics, as summarized in

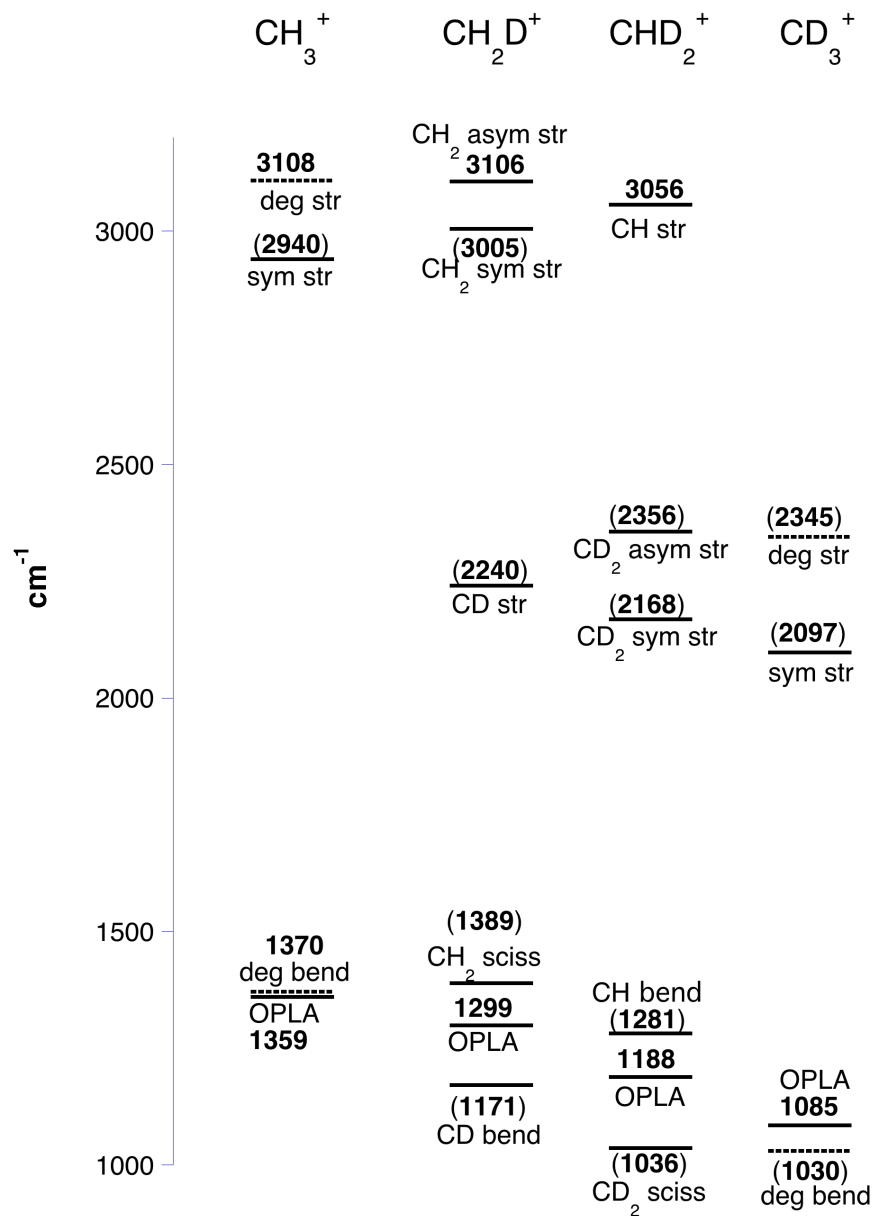


Figure 1: Diagram showing the fundamental vibrations of methyl cation isotopologues. The experimental vibrational frequencies are listed when available. Theoretical values are given in parenthesis. Dotted lines correspond to degenerate modes of vibration. OPLA stands for "Out of Plane Large Amplitude" mode. Adapted from Brum *et al.*, 1993.[?]

Irikura, 2007,² their estimates, computations and experimental corrections are much less obvious for polyatomics (Csonka *et al.* 2005).² Using a fourth-order expansion of the potential energy, the second order perturbative expression of the vibrational energy of asymmetric tops can be expressed as:²

$$E_n = \chi_0 + \sum_i g_i v_i^0 (n_i + \frac{1}{2}) + \sum_i \sum_{j < i} g_i g_j \chi_{ij} (n_i + \frac{1}{2})(n_j + \frac{1}{2}) \quad (1)$$

where v_i^0 is the harmonic frequency and the anharmonic constants χ_{ij} are simple functions of the second, third and semi-diagonal fourth energy derivatives w.r.t. normal modes. One can then derive the expressions of the fundamental vibrational frequencies v_i and ZPE :

$$v_i = v_i^0 + 2\chi_i + \frac{1}{2} \sum_{j \neq i} \chi_{ij} \quad (2)$$

and

$$ZPE = \chi_0 + \frac{1}{2} \sum_i (v_i^0 + \frac{1}{2} \chi_{ii} + \sum_{j < i} \frac{1}{2} \chi_{ij}) \quad (3)$$

Different methods have been proposed to obtain improved ZPE's by combing the formulae including harmonic vibrations and fundamental vibrations. We follow the recent prescription² for computing the ZPE of the methylium molecular ion:

$$ZPE_{vib} = \sum_i g_i (\frac{3}{8} h v_i^0 + \frac{1}{8} h v_i) \quad (4)$$

The ZPEs of the deuterated substitutes of CH_3^+ are estimated from the formula including the fundamental frequencies only, as no other information is available:

$$ZPE'_{vib} = \sum_i g_i \frac{1}{2} h v_i \quad (5)$$

We also compute the corresponding value for CH_3^+ . The values are reported in Table 2. The resulting accuracy is difficult to estimate and the two values displayed for CH_3^+ , differing by an amount of $\sim 69 \text{ cm}^{-1}$, reflect this issue.

CH_3^+ has a planar D_{3h} structure and, as such, the ground rotational (ortho) level 0_{00} is forbidden, as in the case of H_3^+ , due to Fermi statistics. The first rotational level of CH_3^+ is then the para form level 1_1 . The corresponding rotational energy terms are expressed as :

$$E_{J,K} = BJ(J+1) + (C-B)K^2 \quad (6)$$

With the values given in Table 1, the first energy terms of level 1_1 (para) and 1_0 (ortho) are respectively 14.08 and 18.72 cm^{-1} , measured from the ground vibrational term. This additional rotational energy term is quoted explicitly for para and ortho forms of CH_3^+ . We also display the ZPE values of H_2 , H_2O , HCN and deuterated isotopologues which will be used further to determine the energy released in possible deuterium exchange reactions. These values include the anharmonic contribution.

Table 2: Zero Point Energies in cm^{-1} .

	p- CH_3^+	o- CH_3^+	CH_2D^+	CHD_2^+	CD_3^+
ZPE (Eq. 4)	$6834.5 + 14.08$	$6834.5 + 18.72$			
ZPE' (Eq. 5)	$6903.5 + 14.08$	$6903.5 + 18.72$	6105	5542.5	4966

	H_2	HD	D_2	H_2O	HDO	HCN	DCN
ZPE	$2179.3^?$	$1890.3^?$	$1546.5^?$	$4638.3^?$	$4022.8^?$	$3479.2^?$	$2883.9^?$

Fractionation reactions

Significant enhancements of deuterated molecules compared to the elemental D/H ratio of about 1.5×10^{-5} have been found towards cold, dense and CO-depleted molecular cores.^{????} Indeed, the observed $\text{HCO}^+/\text{DCO}^+$ and $\text{N}_2\text{D}^+/\text{N}_2\text{H}^+$ ratios reach high values only in the coldest clouds and the deuterated variants are practically unobservable in a warm cloud such as OMC-1,[?] in fair agreement with gas-phase chemistry predictions. DCO^+ and N_2D^+ are essentially formed from the reaction of H_2D^+ with CO and N_2 , so that the $\text{DCO}^+/\text{HCO}^+$ and $\text{N}_2\text{D}^+/\text{N}_2\text{H}^+$ ratios reflect

essentially the $\text{H}_2\text{D}^+ / \text{H}_3^+$ ratio, which decreases rapidly with temperature, as deuterium is loosely bound in the H_2D^+ molecular ion. The exothermicity of the formation reaction via $\text{H}_3^+ + \text{HD}$ has a value of about 230 K and the presence of ortho- H_2 reduces drastically the barrier of the backward reaction as discussed in Pagani *et al.*, 2009.[?]

It has been recognized quite early that deuterium enrichment could also proceed via fractionation reactions of CH_3^+ with HD.[?] The exothermicity of this reaction was then estimated to be of the order of 300 K. Smith and Adams[?] subsequently derived a value of 370 K from an experimental study at low temperatures. This same value of 370 K has been used in later studies for reactions between CHD_2^+ and HD, when multiply deuterated molecules have been introduced in chemical models,[?] following their first detection in the interstellar medium.[?] We revisit the possible fractionation reactions involving $\text{CH}_{3-n}\text{D}_n^+$ in the light of recent ion-molecule studies[?] and selection rules in ortho/para transitions summarized in Oka, 2004,[?] involving conservation of the total nuclear spin. We display in Table 3 the different fractionation reactions and measured reaction rate coefficients at two different temperatures. We also report our computed exothermicities ΔE , obtained from the previously determined ZPEs (Table 2) using fundamental vibrational frequencies: For an exothermic reaction $R_1 + R_2 \rightarrow P_1 + P_2$, the corresponding exothermicity is given by:

$$\Delta E = ZPE(R1) + ZPE(R2) - ZPE(P1) - ZPE(P2) \quad (7)$$

The exothermicities involved in $\text{CH}_{3-n}\text{D}_n^+$ reactions with HD are typically larger than 300 K as previously reported, and we find that the first reaction of CH_3^+ with HD even has an exothermicity close to 650 K, about a factor of 2 larger than the previous estimates, increasing the formation efficiency of CH_2D^+ in warm conditions. The main uncertainty arises from the spectroscopic constants of CH_2D^+ , where only fundamental vibration frequencies have been derived. Similar values are obtained in Parise *et al.*, 2009[?] based on ZPE values from older theoretical values of vibrational frequencies reported in DeFrees & McLean, 1985.[?]

The measurements by Asvany *et al.*[?] showed that the reaction rate coefficient of para- CH_3^+ in para- H_2 buffer gas is much smaller than the value obtained with a He buffer gas involving

Table 3: Rate coefficients for various deuterium exchange reactions and exothermicities (computed from ZPEs) of the forward reaction.

reaction		exothermicity (K)	rate coefficient of the forward reaction (cm ³ s ⁻¹)		
			15K	80K	
CH ₃ ⁺ + HD	⇌	CH ₂ D ⁺ + H ₂	654	1.65 ± 0.1 (-9) ^{? a}	
CH ₃ ⁺ (para) + HD	⇌	CH ₂ D ⁺ + H ₂ (para)	654	4.0 (-10) ^{? b}	
CH ₃ ⁺ (para) + HD	⇌	CH ₂ D ⁺ + H ₂ (ortho)	483	6.7 (-10) ^{? c}	
CH ₃ ⁺ (ortho) + HD	⇌	CH ₂ D ⁺ + H ₂ (para)	660	1.9 (-10) ^{? c}	
CH ₃ ⁺ (ortho) + HD	⇌	CH ₂ D ⁺ + H ₂ (ortho)	489	1.3 (-9) ^{? c}	
CH ₃ ⁺ + HD	⇌	CH ₂ D ⁺ + H ₂	654		1.1 (-9) [?]
CH ₂ D ⁺ + HD	⇌	CHD ₂ ⁺ + H ₂	393	1.59 ± 0.1 (-9) [?]	7.4 (-10) [?]
CHD ₂ ⁺ + HD	⇌	CD ₃ ⁺ + H ₂	414	1.50 ± 0.1 (-9) [?]	6 (-10) [?]
CH ₃ ⁺ + D ₂	⇌	CHD ₂ ⁺ + H ₂	969		6.6 (-10) [?]
CH ₃ ⁺ + D ₂	⇌	CH ₂ D ⁺ + HD	575		4.4 (-10) [?]
CH ₂ D ⁺ + D ₂	⇌	CD ₃ ⁺ + H ₂	728		3 10(-10) [?]
CH ₂ D ⁺ + D ₂	⇌	CHD ₂ ⁺ + HD	315		9 (-10) [?]
CHD ₂ ⁺ + D ₂	⇌	CD ₃ ⁺ + HD	335		7.4 (-10) [?]
CH ₃ ⁺ + HDO	⇌	CH ₂ D ⁺ + H ₂ O	178		
CH ₃ ⁺ + DCN	⇌	CH ₂ D ⁺ + HCN	207		

Values in parentheses refer to power of 10.

^a : He buffer gas, pure HD target

^b : para-CH₃⁺ in para-H₂ buffer gas

^c: present derivation from branching ratios displayed in Table 4. See text.

pure HD target. We introduce the reactions between CH_3^+ and HD involving specific para/ortho forms of CH_3^+ and H_2 and derive the corresponding rate coefficients by including the expected branching ratios obtained from the selection rules given in Oka, 2004.[?] The corresponding values are summarized in Table 4 and differ slightly from those previously assumed by Walmsley *et al.*, 2004[?] for the $\text{H}_3^+ + \text{HD}$ reaction.

Table 4: Branching ratio of the $\text{CH}_3^+ + \text{HD} \rightarrow \text{CH}_2\text{D}^+ + \text{H}_2$ reaction.

	(o- CH_2D^+ , o- H_2)	(o- CH_2D^+ , p- H_2)	(p- CH_2D^+ , o- H_2)	(p- CH_2D^+ , p- H_2)
p- $\text{CH}_3^+ + \text{HD}$	3/8	1/4	1/4	1/8
o- $\text{CH}_3^+ + \text{HD}$	6/8	1/8	1/8	0

As an example, the derived rate coefficient of the p- CH_3^+ in o- H_2 is 5/3 that of p- CH_3^+ in p- H_2 , as we do not discriminate the ortho/para forms of CH_2D^+ . The other values are obtained by using the total rate coefficient measured in pure HD and assuming that para and ortho CH_3^+ are in equal proportions in the experiment. Then, $k_{(o-\text{CH}_3^+ + \text{HD} \rightarrow \text{CH}_2\text{D}^+ + o-\text{H}_2)} = \frac{7 \times 4}{22} \times 1.05 \times 10^{-9} \text{ cm}^3 \text{ s}^{-1}$ and $k_{(o-\text{CH}_3^+ + \text{HD} \rightarrow \text{CH}_2\text{D}^+ + p-\text{H}_2)} = \frac{4}{22} \times 1.05 \times 10^{-9} \text{ cm}^3 \text{ s}^{-1}$.

As it has been found that CH_3^+ does not react with H_2O , nor with HCN ,[?] we consider possible deuterium exchange reactions of CH_3^+ with HDO and DCN , which are also displayed in Table 3. The deuterium exchange reaction between CH_3^+ and HDO is found exothermic whereas ?[?] quote it to be endothermic by a similar amount. We also find that the reaction between CH_3^+ and DCN is exothermic. These last reactions have not been studied in the laboratory, but they may contribute to the general balance of deuterium exchange reactions in moderately warm environments.

Observations

CH_2D^+ has several transitions which can be studied from the ground and Figure 2 lists the first energy levels and the corresponding transitions as reported in the CDMS catalog. Searches of the 490.0 GHz fundamental ortho transition of CH_2D^+ were performed in May 2007 using the Caltech

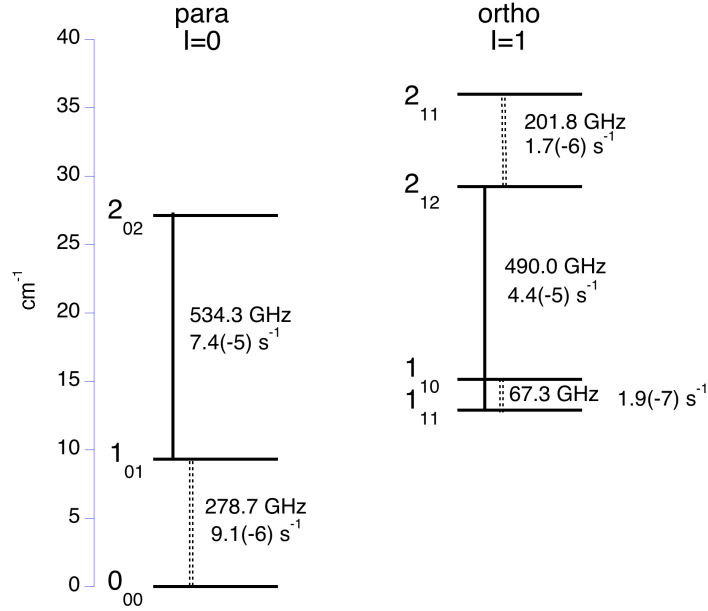


Figure 2: Energy diagram of CH₂D⁺. Rotational frequencies are listed as well as Einstein coefficients. Full lines refer to laboratory measured transitions.⁷ Double dotted lines correspond to theoretical predictions derived from fitting the experimental available spectrum with model Hamiltonians. $x(y)$ stands for $x \times 10^y$.

Submillimeter Observatory (CSO) on Mauna Kea, Hawaii. No positive detections were obtained towards the low-mass protostar IRAS 16293-2422 and the prestellar core IRAS 16293-2422E, with total on source integration times of 70 and 39 minutes respectively. The corresponding receiver was no longer available during the subsequent observing runs.

Then, spectroscopic observations of the 278.7 and 201.7 GHz rotational lines of CH₂D⁺ in Orion IRc2 (RA(2000) = 05:35:14.2, DEC(2000)=-5:22:36, $v_{LSR} = 9 \text{ km s}^{-1}$) were carried out in 2009 January–February using the 230 GHz facility receiver and spectrometers of the CSO. The weather conditions were good to average, characterized by a 225 GHz zenith opacity of $\sim 0.06 - 0.12$. The CSO beam size at the two frequencies is $\sim 26''$ and $36''$, respectively, and the main beam efficiency, as determined from total power observations of Saturn, was $\sim 65\%$ and 70% respectively. The 278.7 GHz spectra were taken in the position-switching mode, with the reference position 10 arc min away in right ascension. The velocity resolution of the FFT spectrometer at the frequencies studied here is about 0.066 and 0.09 km s^{-1} , respectively. Pointing was determined by frequent total power observations of the dust continuum in Orion IRc2. Additional spectroscopic

observations have been performed with the IRAM 30m telescope, in which we recovered the same spectral features as those detected with the CSO. Observations were performed in July 2009 (201 GHz) and in February and November 2010 (278 GHz and DCN J=2-1), with variable weather conditions at high spectral resolution. We used the Eight MIxer Receivers (EMIR) together with the VErsatile SPectrometer Array (VESPA), providing 80 kHz of spectral resolution (0.12 and 0.08 km s⁻¹ at 201 and 278 GHz, respectively). All the observations were taken in the Wobbler switching mode, with a secondary throw of 4'. Beam sizes at 201 and 278 GHz are ~11" and 9" respectively, corresponding to main beam efficiencies of ~57% and 46%.

Corresponding spectra at 279 GHz and 201 GHz taken at the central (0,0) position are shown in Figure 3, where the baselines have been subtracted. The first row displays spectra obtained from CSO. The total on-source integration time is 125 minutes, with an average system temperature of 330 K for the 279 GHz transition. The LO frequency has been optimized to position the CH₂D⁺ line in-between strong lines from the image sideband. The 201.7 GHz frequency is close to the lower end of the tuning range of the receiver. The system was therefore less stable and the spectra at this frequency were taken in the beam-switching mode with a secondary chopper throw of 4 arc min. The average system temperature is then 525 K and the corresponding integration time is 122 minutes. The second row displays the IRAM observations. Total on-source integration times are 5.8 hrs for both transitions with system temperatures ranging between 160 to 400 K and opacities of 0.06–0.3 at 279 GHz. The parameters obtained from the gaussian fits are reported in Table 5 and are remarkably consistent in terms of line position and width between the two telescopes. We also report the frequency values derived by Amano[?] who was able to detect pure rotational transitions at high frequencies, providing strong constraints on the subtle distortion constants involved in the model Hamiltonian. These values differ by less than 100 kHz from those reported in CDMS, which are deduced from high spectral resolution laser induced infrared spectra.^{??} The frequency agreement between our "observed" value and these predictions is excellent. Thanks to the higher spatial resolution available at IRAM and the higher signal to noise ratio, the 201 GHz feature may consist of 2 velocity components, the narrower one consistent with the value derived for the

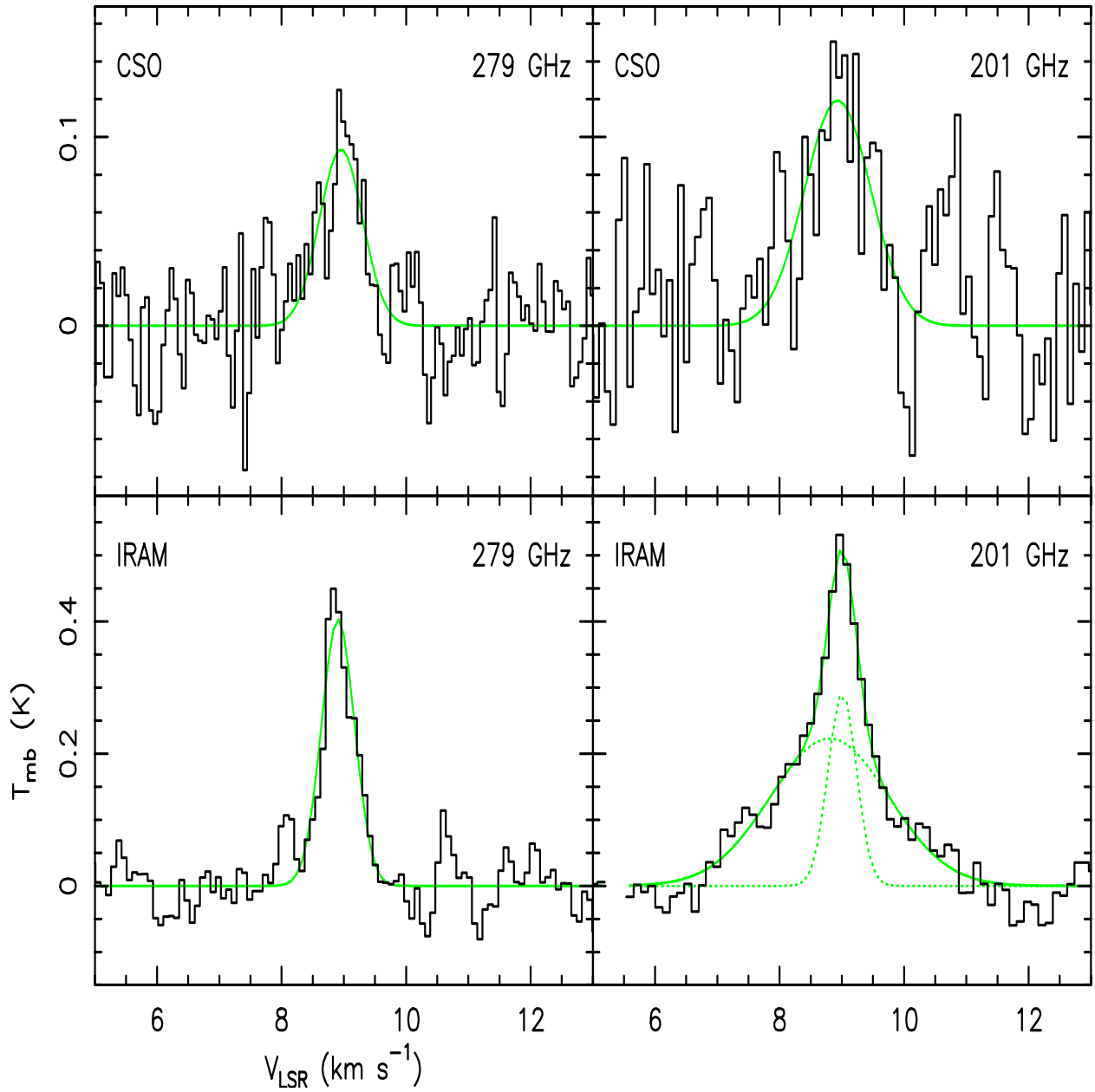


Figure 3: Spectra at the frequencies of the 279 GHz and 201 GHz CH_2D^+ lines toward Orion IRc2. The upper (lower) panels show the spectra obtained at CSO (IRAM), where baselines have been removed. The green lines display the corresponding Gaussian fits.

Table 5: Parameters derived from the CSO and IRAM spectroscopic observations.

Frequency MHz	Transition	Telescope	Velocity km/s	width km/s	Area K km/s
278691.8 ⁽¹⁾	1 ₀₁ - 0 ₀₀ (para)	CSO	8.946	0.748	0.073
		IRAM	8.909	0.636	0.269
201754.2 ⁽²⁾	2 ₁₁ - 2 ₁₂ (ortho)	CSO	8.933	1.25	0.159
		IRAM	9.007	0.534	0.166
		IRAM	8.803	2.23	0.530

⁽¹⁾ the corresponding frequency reported by Amano[?] is 278691.656 (26) MHz.

⁽²⁾ the corresponding frequency reported by Amano[?] is 201753.947(70) MHz.

278 GHz transition. Indeed, the Orion-IRc2 source is heavily congested with lines and great care is required before claiming a detection. The 201 GHz range is particularly delicate as several methyl formate (E species) transitions occur at a very close frequency (201.75325 GHz), however originating from quite excited levels (E ~ 300K). Si¹⁸O (J=5-4) at 201.7515 is also present[?] and disentangling the various components is beyond the present study.

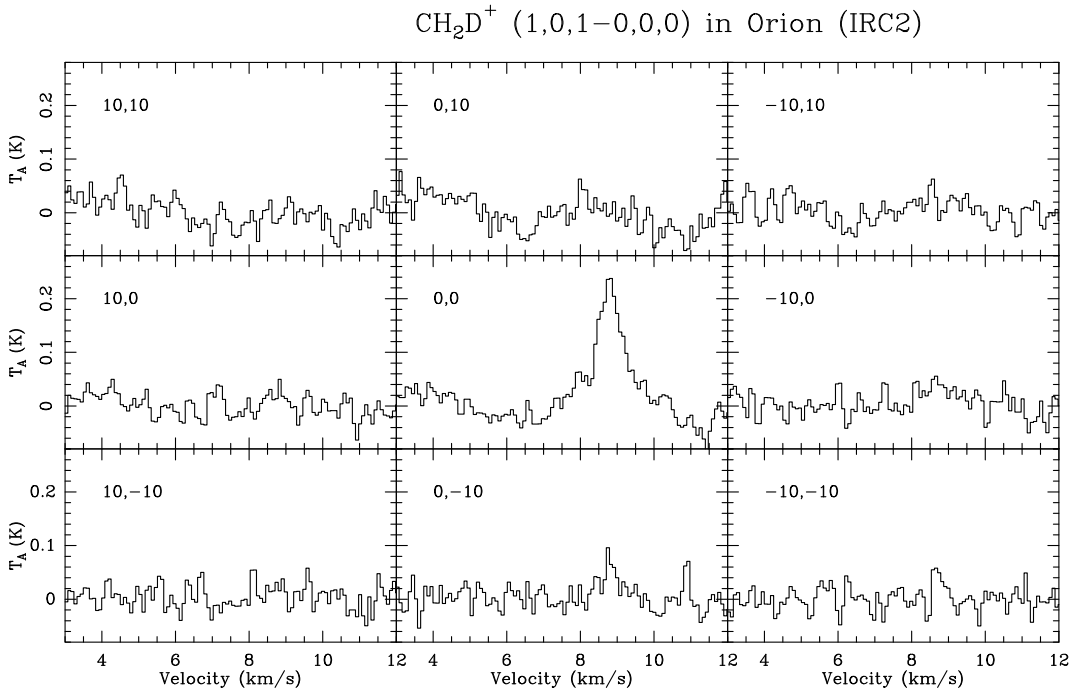


Figure 4: map at 278.7 GHz CH_2D^+ 1₀₁-0₀₀ transition toward Orion IRC2.

DCN (2-1) in Orion (IRC2)

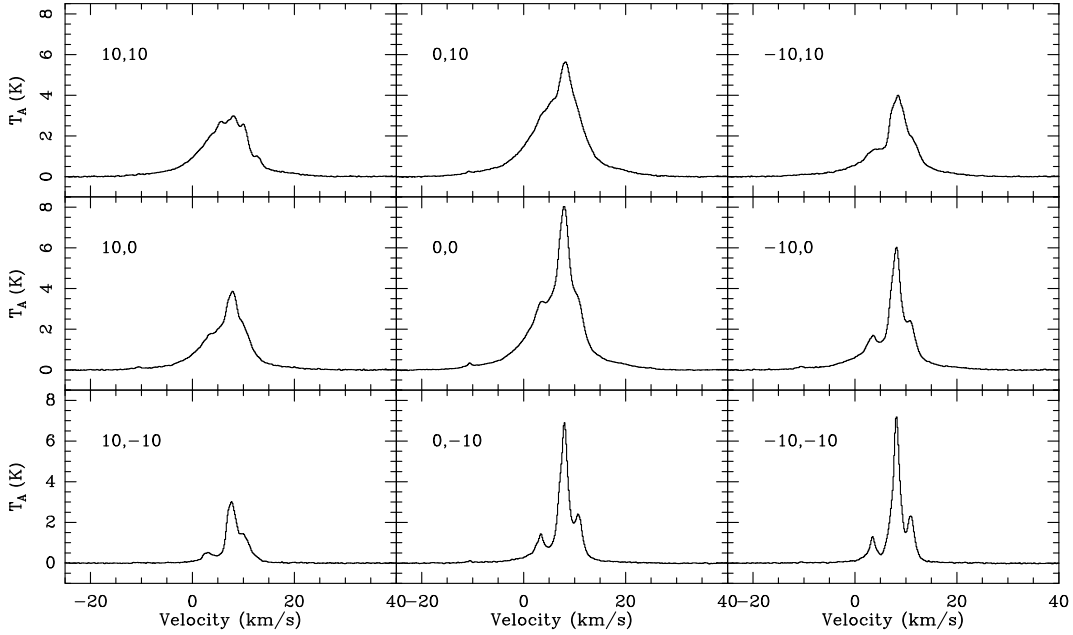


Figure 5: map at 144.8 GHz DCN $J=(2-1)$ transition toward Orion IRC2.

We also performed a map of both 201 and 278 GHz spectral features around the (0,0) position, together with emission from HDCO and DCN with the IRAM 30m telescope. As pointed out earlier, the feature at 201 GHz could be blended with methyl formate emission, thus we only display the maps corresponding to the 278 GHz feature in Figure 4. Total integration times are 5.8 hrs towards the centre, and ~ 1.5 hrs at the other positions of the map. Figure 5 presents emission from DCN $J=2-1$ observed simultaneously. Both maps show a peak at the central position but the 278 GHz feature is much more localized. We thus tentatively conclude from our observations that the carrier of the detected transitions is CH_2D^+ and occupies a very limited region. A FWHM source size of $11.5''$ is required to reproduce the IRAM and CSO spectra at 278 GHz. We explore the possible corresponding observational parameters for other transitions detectable with GBT and Herschel HIFI. Table 6 displays the predictions for the corresponding integrated intensities for different values of the excitation temperature and assuming an ortho to para ratio of 3, as expected in the high temperature limit. The predicted line intensities for the ortho 201 GHz transition are significantly smaller than the observed ones, which suggests a possible blend. A full account of

these spectral features leads to an unrealistically high ortho to para ratio and we thus principally aim at reproducing the para 278 GHz observational parameters, as shown in Table 6. The observed spectra are modeled using the myXCLASS software package ¹ and the column densities are reported in Table 6. Lis et al. ² have mapped the Orion A Molecular cloud at 350 μm and obtained a

Table 6: Integrated intensities of different CH_2D^+ transitions in K km/s : model predictions and corresponding column densities. Observed values are also reported when available.

Telescope	Transition MHz	LTE model			Observed K km/s
		T= 20 K K km/s	T= 30 K K km/s	T= 40 K K km/s	
GBT	67273.574	0.172	0.178	0.197	
IRAM	201754.2	0.061	0.102	0.143	0.166
CSO	201754.2	0.012	0.02	0.029	0.159
IRAM	278691.8	0.271	0.270	0.273	0.271
CSO	278691.8	0.071	0.071	0.072	0.072
HIFI	490012.247	0.059	0.084	0.109	
HIFI	534280.117	0.033	0.051	0.064	
N (ortho)	($\times 10^{13}\text{cm}^{-2}$)	5.67	7.5	10.5	
N (para)	($\times 10^{13}\text{cm}^{-2}$)	1.89	2.5	3.35	
N (total)	($\times 10^{13}\text{cm}^{-2}$)	7.6	10.0	13.9	

maximum flux of 1300 Jy within a 12" beam. With a dust temperature of 55 K and an absorption coefficient of $10\text{ cm}^2/\text{g}$, the resulting H_2 column density is $1.35 \times 10^{24}\text{ cm}^{-2}$. Then, the resulting fractional abundance of CH_2D^+ relative to molecular hydrogen is between 5.6×10^{-11} and 1.0×10^{-10} . The derived value is based on the 278 GHz para transition.

Astrochemical models

Astrochemical models, in which one solves the coupled differential equations describing the time evolution of the various chemical species resulting from formation/destruction chemical processes at one given temperature and density, allow to check the relevance of the proposed identification.

¹available at <http://www.astro.uni-koeln.de/projects/schilke/XCLASS>

To address this point, we amended the chemical network used in Pagani *et al.*, 2011, 2012,² where ortho/para forms of H_2 , H_2^+ , H_3^+ and all their deuterated substitutes are considered separately in the chemical reactions. We introduced para/ortho forms of CH_3^+ in order to take into account their different behavior in the presence of HD, as discussed previously and shown in Table 3. The effect of the small energy difference between the two lowest para and ortho levels of CH_3^+ ($4.6 \text{ cm}^{-1} \sim 7 \text{ K}$) is, however, negligible in comparison with the exothermicities involved in the reactions. This differs from ortho-hydrogen, which has an energy of 118.5 cm^{-1} ($\sim 170.5 \text{ K}$) above the para level and can significantly reduce the deuterium fractionation efficiency in the $H_3^+ + HD \rightleftharpoons H_2D^+ + H_2$ reaction, as first pointed out by Pagani *et al.*² We included the recent values of the dissociative recombination rates and branching ratios of CH_3^+ , as measured by Thomas *et al.*² in the heavy storage ring CRYRING in Stockholm. Reactions involving nitrogen have been studied recently² as advertised in the KIDA database² and the corresponding rate coefficients have been modified accordingly. Then, the chemical network includes 220 atomic and molecular species (where para(ortho) form is counted as a molecular species) and 4024 chemical reactions.

Figure 6 displays the time evolution of selected fractional molecular abundances, as well as the corresponding deuterium fractionation ratios for $T = 50\text{K}$ and a molecular hydrogen density of 10^5 cm^{-3} . We find that the time evolution profiles of H_2CO and CH_3^+ exhibit a maximum around several 10^4 years, the so-called "early time" value,² for which the value of the total CH_3^+ fractional abundance is about 4×10^{-10} , about two orders of magnitude higher than the steady state value, which is reached when the molecular fractional abundance becomes independent of the time scale. We have verified that the location of the maxima and the corresponding fractional abundance values are similar, regardless of the initial condition (initial atomic or molecular hydrogen). The steady state values are reached at different times, depending on the considered molecules and are found to be independent on the initial conditions, as expected. The deuterium fractionation ratios at the early time peak are also significantly higher than the values at steady state, except for H_2CO and CH_3^+ where the ratios exhibit a small increase from the early time values up to steady state.

²available at <http://kida.obs.u-bordeaux1.fr/>

In order to test the density and temperature dependences, we display steady state results for density values $n(\text{H}_2) = 10^4$ and 10^5 cm^{-3} , at 3 different temperatures corresponding to medium warm environments in Table 7, in the range of physical conditions thought to be present in the Orion IRc2 region. The steady state ortho-to-para ratio of H_2 is found to be slightly smaller, but close to its temperature equilibrium value, labelled as ETL. Ortho and para CH_3^+ have very similar fractional abundances. The deuterium ratio in CH_3^+ is of the order of 10 %, even at $T = 60 \text{ K}$; however, the fractional abundances are quite small and close to a detectable limit. The values decrease with increasing densities as well, following the trend of the fractional ionization. CH_2D^+ may also be used to transfer deuterium to HCN , H_2CO , HCO^+ , ... via its reaction with atomic oxygen and nitrogen, as emphasized in Roueff *et al.*, 2007,² Parise *et al.*, 2009² and offers an alternative way of deuteration via gas phase processes in medium warm environments. As expected, the ratio of deuterated molecules compared to the main isotopologue is a decreasing function of temperature. The deuteration ratios of HCN , HCO^+ and N_2H^+ are in the $10^{-3} - 10^{-4}$ range, whereas that of H_2CO is several percent. However, as the fractional abundance of HCN is about fifty times higher than that of H_2CO , even a smaller deuterium fractionation is observable, as shown in the DCN map displayed in Figure 5. These results can support a possible detection of the CH_2D^+ molecular ion under quite specific conditions: as the fractional abundances are small, a large column density of molecular hydrogen is required, a range of temperatures between 40 - 60 K is adequate, and evolution times of several ten thousands years are propitious. Such requirements may be met in Orion IRc2.

Conclusions

We have presented a careful analysis of the gas phase chemistry associated with CH_3^+ and its deuterated variants. ZPEs of the various deuterated isotopologues have been derived in the light of recent spectroscopy experiments and quantum chemical calculations. The role of anharmonicity effects is only included for CH_3^+ , for which information is available. The significant exothermicity-

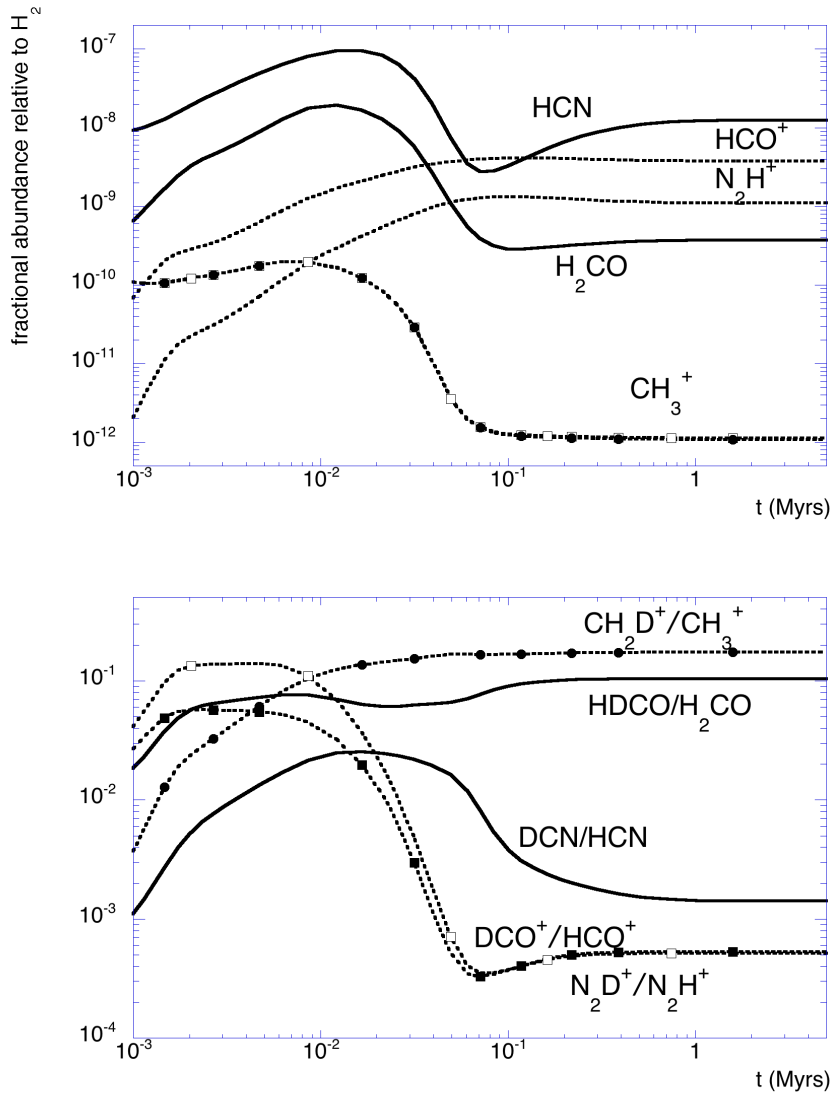


Figure 6: Time evolution results corresponding to $T = 50$ K and $n(H_2) = 10^5 \text{ cm}^{-3}$.

Upper panel: time evolution of fractional abundances of H_2CO , HCN, CH_3^+ (para (open squares) and ortho (full circles)), HCO^+ and N_2H^+ . Neutrals are displayed as full lines, ions as dotted lines.

Lower panel : corresponding deuterium fractionation ratios. full circles: CH_2D^+/CH_3^+ ; open squares: DCO^+/HCO^+ ; full squares: N_2H^+/N_2D^+ .

ties involved in the deuterium exchange reactions with HD allow an efficient deuterium enrichment of CH_3^+ . However, as CH_3^+ may also react with H_2 in a slow (but not insignificant and not well known) radiative association reaction, its fractional abundance remains low, but exhibits a suggestive maximum at the early time peak during the time evolution. We have reported our observational searches of CH_2D^+ in the Orion IRc2 region. Two spectral features detected at 201.7542 and 278.6918 GHz respectively, may correspond to the CH_2D^+ molecular ion. Those values are very close to the frequencies predicted by Amano.[?] However, the feature at 201 GHz may be blended with methyl formate and Si^{18}O .[?] The feature at 278 GHz is cleaner. However, one single spectral feature is obviously not adequate to claim a secure identification. We also predict integrated intensities for other transitions which may become accessible in the near future. If real, the CH_2D^+ source in Orion is extremely localized and should be at relatively moderate temperatures below $\sim 50\text{K}$, given the reported line width of less than 1 km s^{-1} . In addition, chemical modeling can positively corroborate such a detection, more favourably when time dependent effects are invoked. In spite of the observational challenges, the updated chemical analysis performed here should help understanding the formation/destruction mechanisms of this puzzling molecular ion and constrain the possible role of gas phase chemistry in the deuteration of interstellar molecules in warm environments.

Acknowledgement

This work has greatly benefited from different aspects of Oka's contributions in various areas. This research is partly based upon work at the Caltech Submillimeter Observatory, which is operated by the California Institute of Technology under cooperative agreement with the National Science Foundation (AST-0838261) and also on observations obtained with the IRAM-30 m telescope. IRAM is supported by INSU/CNRS (France), MPG (Germany), and IGN (Spain). Part of the work has been done when D. Lis was visiting LERMA as invited professor at the Physics Department of Ecole Normale Supérieure.

Table 7: Steady state fractional abundances relative to H₂ for different values of n(H₂) and temperature.

Temperature n(H ₂) cm ⁻³	40 K		50 K		60 K	
	10 ⁴	10 ⁵	10 ⁴	10 ⁵	10 ⁴	10 ⁵
H ₂ (para)	0.899	0.898	0.791	0.789	0.681	0.678
H ₂ (para) ETL	0.873	0.873	0.703	0.703	0.475	0.475
H ₂ (ortho)	0.101	0.102	0.209	0.211	0.319	0.322
H ₂ (ortho) ETL	0.127	0.127	0.297	0.297	0.525	0.525
H ₃ ⁺ (para)	2.92(-8)	4.77(-9)	2.91(-8)	4.83(-9)	2.91(-8)	4.89(-9)
H ₃ ⁺ (ortho)	1.45(-8)	2.37(-9)	1.62(-8)	2.71(-9)	1.76(-8)	2.96(-9)
H ₂ D ⁺ (para)	4.92(-11)	7.95(-12)	1.80(-11)	2.96(-12)	9.99(-12)	1.66(-12)
H ₂ D ⁺ (ortho)	6.19(-11)	1.01(-11)	3.10(-11)	5.12(-12)	2.08(-11)	3.48(-12)
D ₂ H ⁺ (ortho)	7.04(-13)	1.16(-13)	1.24(-13)	2.11(-14)	4.40(-14)	7.51(-15)
D ₂ H ⁺ (para)	1.68(-13)	2.72(-14)	3.28(-14)	5.39(-15)	1.24(-14)	2.06(-15)
CH ₃ ⁺ (para)	2.22(-11)	9.56(-13)	2.38(-11)	1.12(-12)	2.59(-11)	1.35(-12)
CH ₃ ⁺ (ortho)	2.14(-11)	8.98(-13)	2.31(-11)	1.08(-12)	2.63(-11)	1.45(-12)
CH ₂ D ⁺	4.15(-12)	2.79(-13)	4.94(-12)	3.84(-13)	3.79(-12)	2.76(-13)
HCN	7.74(-8)	1.58(-8)	7.17(-8)	1.24(-8)	6.67(-8)	9.96(-9)
DCN/HCN	1.4(-3)	1.8(-3)	8.4(-4)	1.4(-3)	4.9(-4)	8.5(-4)
H ₂ CO	1.75(-9)	4.02(-10)	1.54(-9)	3.71(-10)	1.37(-9)	3.39(-10)
HDCO / H ₂ CO	0.085	0.12	0.071	0.10	0.043	0.055
HCO ⁺	7.38(-9)	3.13(-9)	8.51(-9)	3.76(-9)	9.56(-9)	4.36(-9)
DCO ⁺ / HCO ⁺	1.4(-3)	1.1(-3)	6.7(-4)	5.1(-4)	4.2(-4)	3.1(-4)
N ₂ H ⁺	1.39(-9)	9.03(-10)	1.65(-9)	1.10(-9)	1.92(-9)	1.28(-9)
N ₂ D ⁺ / N ₂ H ⁺	1.4(-3)	1.25(-3)	6.0(-4)	5.3(-4)	3.4(-4)	3.1(-4)

The elemental abundances are [D]/[H] = 1.6×10^{-5} , [C]/[H] = 7.0×10^{-6} , [O]/[H] = 2×10^{-5} , [N]/[H] = 10^{-5} , [S]/[H] = 1.8×10^{-7} and a representative metal [M]/[H] = 1.5×10^{-8} . Values in parentheses refer to power of 10.